Acta Materialia 105 (2016) 84–93

Contents lists available at ScienceDirect

Acta Materialia

journal homepage: www.elsevier.com/locate/actamat

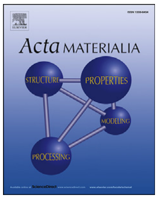

Full length article

Microstructure evolution during internal reduction of polycrystalline nickel-doped yttria-stabilized zirconia

Amy Morrissey [a], James R. O'Brien [b], Ivar E. Reimanis [a, *]

[a] Colorado Center for Advanced Ceramics, Metallurgical and Materials Engineering Department, Colorado School of Mines, Golden, CO 80401, USA
[b] Off Grid Research, 6501 Goodwin Street, San Diego, CA 92111, USA

ARTICLE INFO

Article history:
Received 29 July 2015
Received in revised form
7 November 2015
Accepted 3 December 2015
Available online 24 December 2015

Keywords:
Reduction
Yttria-stabilized zirconia polycrystal
Nickel
Nanoparticles
SQUID magnetometry

ABSTRACT

The nucleation and growth of metallic particles within metal-doped oxides in reducing conditions is relevant to the processing of materials for catalysis, fuel cells, and structural applications. Here, the precipitation of metallic nickel during the internal reduction of nickel-doped yttria stabilized zirconia is studied with electron microscopy and SQUID magnetometry. It is shown that the microstructure evolution proceeds in three distinct stages, each with its own kinetics description, dependent on the porosity and grain size. 0.5 M percent NiO doped YSZ was synthesized, sintered, pressed into pellets, and then exposed to 1000 °C in 2% H_2 for various times. Metallic Ni^0 particles (>100 nm) are first formed in pores connected to grain boundaries; subsequently, metallic Ni^0 particles (20–50 nm) precipitate at grain boundaries; and finally, superparamagnetic Ni^0 particles (<10 nm) form within the bulk YSZ grains. The transitions between stages depend upon concentration gradients and electrostatic potentials that act upon the relevant transporting species, namely oxygen vacancies, electrons, nickel ions and zirconium vacancies.

1. Introduction

The process of internal reduction, sometimes also referred to as partial reduction, is a convenient and potentially powerful way to make metal-ceramic composites for diverse applications [1–6]. In internal reduction, a mixed metal oxide solid solution is exposed to a reducing environment at elevated temperature such that the most noble of the metal cations reduces its oxidation state, leading to the precipitation of a second phase within the less noble metal oxide. When the oxygen partial pressure is low enough to form a metal, but not so low as to reduce the parent oxide, the resulting microstructure leads to a metal particulate reinforced ceramic with a microstructure that may exhibit enhanced structural, catalytic or other functional properties [7–11]. The process is more complex than direct reduction where by metal oxide particles in a ceramic matrix directly convert to metal particles [12]. Accordingly, the mass transport and kinetics describing the process are distinctly different from those of direct reduction.

The mechanism for internal reduction was first described by Schmalzried [13,14]. Typically, it occurs by the growth of a reaction zone from the surface to the interior, described by parabolic kinetics, and rate-limited by the diffusion of cations, anions, or electronic charge carriers through the thickness of the reacted zone. The process has been well-described in homogeneous systems such as glass and in single crystal oxides [15–20]. However, complexities are introduced in the presence of microstructural features such as grain boundaries and porosity, as they introduce space charge layers and additional pathways for diffusion that may modify nucleation and growth conditions [21,22]. In highly doped systems, like yttria-stabilized zirconia (YSZ), the intrinsic defect concentrations from the dopant may be several orders of magnitude higher than the extrinsic defect concentrations that are introduced by the externally applied chemical potential gradient [23]. Particularly when high concentrations of intrinsic defects exist, the mass transport of charged species is dominated by an electrical potential [24].

Nickel-YSZ composites have been extensively studied due to their potential use in catalyst systems as well as their use as anodes in solid oxide fuel cells (SOFCs) [25–30]. For SOFCs, NiO is typically mixed with YSZ, co-fired in air to partial density, and then exposed to a reducing atmosphere to directly convert NiO to metallic Ni (Ni^0). Invariably, some NiO dissolves in YSZ during the air firing step. Subsequently, Ni^0 exsolves during the reduction step via a

---

* Corresponding author.
E-mail address: reimanis@mines.edu (I.E. Reimanis).

http://dx.doi.org/10.1016/j.actamat.2015.12.005
1359-6454/

process of internal reduction. In studies with compositions below or near the solubility limit of NiO in YSZ (about 2 M percent [31,32]) it is possible to produce nanometer size dispersions of Ni^0 in YSZ [33,34]. Depending on the starting YSZ microstructure and the specific reducing conditions, the possible size and distribution of Ni^0 particles one can engineer is potentially enormous. The present study examines internal reduction in a polycrystalline NiO doped-YSZ containing a small amount (~5%) of porosity. 10 YSZ (10 M percent Y_2O_3 in Ref. ZrO_2) was chosen over lower amounts of Y_2O_3 to ensure stability of the cubic phase [35]. 0.5 M percent NiO was chosen because it is well below the solid solubility limit, yet high enough to facilitate detection by electron microscopy and magnetometry. It is shown that three distinct stages of internal reduction occur.

2. Experimental procedure

Specimens in this study were prepared by sintering high purity powders that were synthesized by chemical methods described elsewhere [36]. All compositions were 0.5 mol % NiO in 10 mol % Y_2O_3 stabilized ZrO_2 (10YSZ). Pellets 19 mm in diameter and 4 mm thick were formed in a stainless steel die with a uniaxial press (Carver, Inc., Wabash, IN, USA). The pellets were buried in 0.5 M percent NiO-doped 10YSZ powders in high purity (99.8%) alumina (CoorsTek, Golden, CO, USA) containers at 3 °C min^{-1} to 1500 °C for 4.5 h in air, conditions which result single phase YSZ with nickel completely in solid solution or as ions at internal interfaces, such as grain boundaries or pore surfaces. Magnetometry measurements reveal that no nickel exists as an ordered oxide; only disordered Ni^{2+} ions are present [32]. The density was measured to be 95.6% theoretical as measured by the Archimedes method. X-ray diffraction confirmed that the as-sintered material was single phase cubic zirconia [36]. The grain size was measured by the linear intercept method on SEM micrographs (Fig. 1) to be 5.3 ± 0.5 μm. The pore size and spacing was quantified with image analysis: the average pore radius is 167 nm ± 81 nm, and the average spacing between pores, based on the density and pore size, is 1.5 μm. Previous research suggests that the pore surfaces are sites for Ni^{2+} ions [37].

Laser pulse atom probe tomography (APT) to characterize the Ni^{2+} ion distribution in as-sintered samples was performed prior to reduction treatments using 40 pJ laser energy and 40 K specimen base temperature (Cameca, LEAP 4000X Si, Gennevilliers Cedex, France). APT specimens from the grain interiors and boundaries were prepared using focused ion beam (FIB) milling (FEI Helios Nanolab 600i, Hillsboro, OR). Data analysis was performed using CAMECA IVAS v.3.2.6. software.

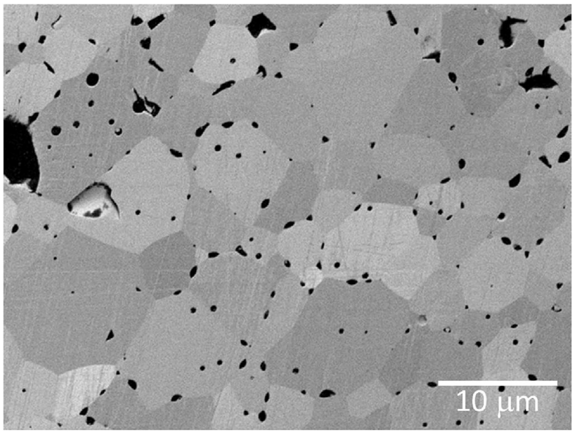

Fig. 1. SEM micrograph showing the as-sintered polycrystalline microstructure of 0.5 M % Ni-doped 10YSZ that contains average grains approximately 5 μm and approximately 5% pre-existing porosity.

Internal reduction experiments were performed on sintered pellets in a high purity (99.8%) alumina reactor tube (CoorsTek, Golden, CO) and tube furnace (ATS, Butler, PA). Gas flow (99.998% Ar or 2% H_2/Ar balance) was regulated with a solenoid valve and mass flow controller calibrated to the gas composition (MKS, Andover, MA). Conditions were chosen to produce a partial pressure of oxygen on the order of 10^{-19} atm, a value calculated to be sufficiently low to lead to internal reduction [38]. The pellet was heated in 100 sccm flowing Ar at 5 °C min^{-1} to 1000 °C. At 1000 °C, the inlet gas was switched to 2% H_2. The inlet gas enters in the back of the reactor tube, flowing over the pellet specimen, and is then exhausted through the face plate. A thermocouple and oxygen sensor is positioned near the pellet inside the reactor tube. The pellets were soaked in 100 sccm flowing 2% H_2 gas for various times (0.5, 5, 10, 25, 50, 66, and 75 h). The measured oxygen partial pressure inside the reactor tube was approximately 10^{-19} atm. Following the reduction hold time, the reactor tube was purged with 100 sccm flowing Ar until a temperature of 50 °C was achieved.

Reduction experiments additional to those describe above were performed at a higher oxygen partial pressure and at lower temperatures. Table 1 summarizes the various conditions. While maintaining constant temperature of 1000 °C, the oxygen partial pressure was increased to approximately 10^{-15} atm by bleeding Ar gas into the reactor tube during the reduction treatment. Two additional experiments were performed at 900 °C and 800 °C while maintaining constant oxygen partial pressure of approximately 10^{-19} atm. Times were 0.5, 5, 10, and 25 h. The emphasis of these additional studies is to understand the effect of oxygen partial pressure and temperature on the reduction reaction.

Pellets were cross-sectioned with a diamond saw, mounted in cold-set epoxy, polished, and observed visually and with optical microscopy. The specimens underwent a change in color from tan to gray upon reduction. The change in color proceeded from the surface towards the center with increase in heat treatment time. The depth of this color change was measured directly on the cross sectioned specimen under a low power optical microscope. The mass of Ni^0 formed in each of the reduced specimens was quantified with superconducting quantum interference device (SQUID) magnetometry (MPMS-7, Quantum Design Inc., San Diego, CA, USA). Direct current (DC) susceptibility moment versus field curves were collected on a 50–100 mg pellect section at 100 K to quantify the saturation magnetization [38]. The diamagnetic response of 10YSZ was subtracted from the overall curve measured at 100 K to extract the ferromagnetic response which arises entirely from Ni^0 [32]. The magnetic moment of metallic Ni^0 is 57.50 emu g^{-1} [39].

The metallic Ni^0 particle size was determined with alternating current (AC) SQUID magnetometry (MPMS-7, Quantum Design Inc., San Diego, CA, USA), as described below and in more detail in the Results section. AC susceptibility curves were collected on a 50–200 mg section of pellet using an AC drive of 7 Hz, 100 μT AC drive amplitude, zero DC field, and scanning temperature from 1.8 K to 250 K [38]. The shape and magnitude of the real, χ', and imaginary, χ'', components versus temperature curves represent a combination of contributions from unreduced Ni^{2+} ions (paramagnetic), reduced metallic Ni^0 single-domain particles (≤ 10 nm, superparamagnetic), and reduced metallic Ni^0 multi-domain particles (>100 nm, ferromagnetic). The characteristic magnetic behavior is well-understood [39]. Deconvolution and modeling of each response contributing to the measured data is detailed in the results section.

Transmission electron microscopy (TEM) images were collected with a 200 kV accelerating voltage TEM (Phillips (FEI) CM200,